DOE BES: DIRECTED ASSEMBLY OF BIO-INSPIRED SUPRAMOLECULAR MATERIALS FOR ENERGY TRANSPORT AND CAPTURE:

Mesoscale Construction of Functional Materials in Hydrodynamic Flows

PI: William L. Wilson and Co-PI: Charles M. Schroeder

Date: 09/02/2018

Final Project Report

Summary of work: The precise engineering of mesoscale structures based on molecular building blocks holds enormous promise to catalyze the development of new functional materials for advanced energy technologies. Bio-inspired and synthetic/bio-hybrid systems can play a key role in this effort due to their inherent programmable function and high degrees of sequence control. Despite recent progress, the ability to precisely control the supramolecular assembly of bio-hybrid molecules remains a central problem in the field. Our research aims to fundamentally understand the assembly mechanism of bio-hybrid materials, specifically focusing on sequence-controlled synthetic pi-conjugated oligopeptides. Moreover, we aim to develop new methods for the directed assembly of materials based on tailored fluid flows to guide the emergent structural, optical, and electronic properties of synthetic pi-conjugated peptides.

Overall, our team has made substantial progress on this project through four major Thrusts:

(1) Understanding the role of kinetics on the assembly process of synthetic π-conjugated peptides.
(2) Probing the role of chemistry on the structural properties of these materials.
(3) Real-time *in situ* investigation of the sol-gel transition and assembly of π-conjugated peptides.
(4) Achieving large-area macroscopic alignment and assembly of these materials.

In the following report, we explain major research progress in each of these research Thrusts.

List of Publications:

1. B. Li, S. Li, Y. Zhou, H. A. M. Ardona, L. R. Valverde, W. L. Wilson, J. D. Tovar, C. M. Schroeder, "Non-equilibrium Self-assembly of π-conjugated Oligopeptides in Solution", *ACS Applied Materials & Interfaces*, 9, 3977-3984 (2017).
2. Y. Zhou, B. Li, S. Li, H. A. M. Ardona, W. L. Wilson, J. D. Tovar, C. M. Schroeder, "Concentration-Driven Assembly and Sol-Gel Transition π-conjugated Oligopeptides", *ACS Central Science*, 3, 986-994 (2017).
3. B. Li, L. R. Valverde, F. Zhang, Y. Zhou, S. Li, Y. Diao, W. L. Wilson, C. M. Schroeder, "Macroscopic Alignment and Assembly of π-conjugated Oligopeptides using Colloidal Microchannels", *ACS Applied Materials & Interfaces*, 9, 41586-41593 (2017).
4. L. Valverde, B. A. Thurston, A. L. Ferguson, W. L. Wilson, "Evidence for Prenucleated Fibrilogenesis of Acid-Mediated Self-Assembling Oligopeptides via Molecular Simulation and Fluorescence Correlation Spectroscopy", *Langmuir*, 34, 7346-7354 (2018).
5. E. Jira, B. Li, and C. M. Schroeder, "Phase Diagrams for Assembled π-conjugated Oligopeptides", in preparation (2018).
6. L. Valverde, B. Li, C. M. Schroeder, W. L. Wilson, "Fluidic Directed Assembly and Real-Time Fluorescence Lifetime Imaging of Synthetic Oligopeptides", in preparation (2018).

**DOE BES support acknowledged in all publications.*

List of Personnel Funded on DOE Award (Paid Participants):

- **Dr. William Wilson** – Principal Investigator, Harvard University
- **Prof. Charles M. Schroeder** – Co-Principal Investigator; Professor and Ray and Beverly Mentzer Faculty Scholar, Department of Chemical & Biomolecular Engineering and Beckman Institute for Advanced Science and Technology, University of Illinois at Urbana-Champaign
- **Amanda Marciel** – Graduate Student, Center for Biophysics and Computational Biology, University of Illinois at Urbana-Champaign. Dr. Marciel successfully defended her Ph.D. in 2015, and she is now a Postdoctoral Fellow with Prof. Matt Tirrell in the Institute for Molecular Engineering at the University of Chicago. Dr. Marciel will be starting as an Assistant Professor of Chemical & Biomolecular Engineering at Rice University in January 2019. Dr. Marciel is first author on 1 publication on the general topic of pi-conjugated peptides (in *Advanced Material*s) that preceded the DOE Award by a few months.
- **Dr. Bo Li** – Postdoctoral Fellow, Department of Chemical & Biomolecular Engineering, University of Illinois at Urbana-Champaign. Dr. Li is first author on 2 publications funded by the Award (two publications in *ACS Applied Materials & Interfaces*), and 2nd author on a third publication funded by the Award (in *ACS Central Science).*
- **Yuecheng Zhou** – Graduate Student, Department of Materials Science & Engineering, University of Illinois at Urbana-Champaign. Mr. Zhou is first author on 1 publication funded by the Award (in *ACS Central Science)*, and 2nd author on a third publication funded by the Award.
- **Lawrence Valverde** – Graduate Student, Department of Materials Science & Engineering, University of Illinois at Urbana-Champaign. Dr. Valverde successfully defended his Ph.D. in January 2018, and he is now a Research Engineer at Intel Corp. in Hillsboro, OR. Dr. Valverde is 1st author on 1 publication funded by the DOE Award (in *Langmuir*), and we are currently writing a manuscript based on Dr. Valverde's research for submission.
- **Bryce Thurston** - Graduate Student, Department of Physics, University of Illinois at Urbana-Champaign. Bryce provided computational modeling of the self-assembly process. This work was coupled with FCS measurements to understand the kinetics of peptide assembly. Mr. Thurston is 2nd author on 1 publication funded by the Award (in *Langmuir*).
- **Ziyuan Song** – Graduate Student, Department of Materials Science & Engineering, University of Illinois at Urbana-Champaign. Ziyuan synthesized a new class of pi-conjugated peptides for this work, but the peptides were not sequence-defined, and we found that they did not assemble into well-ordered structures.
- **Ruibo Wang** - Graduate Student, Department of Materials Science & Engineering, University of Illinois at Urbana-Champaign. Ruibo synthesized a new class of pi-conjugated peptides for this work, but the peptides were not sequence-defined, and we found that they did not assemble into well-ordered structures.
- **Rachael Mansbach** - Graduate Student, Department of Physics, University of Illinois at Urbana-Champaign. Rachel provided computational modeling of the self-assembly process. This work was coupled with FCS measurements to understand the kinetics of peptide assembly.
- **Dr. Hao Chen** – Postdoctoral Fellow, Department of Materials Science & Engineering, University of Illinois at Urbana-Champaign. Hao characterized the structure and physical properties of pi-conjugated peptides.

Thrust 1: Role of kinetics on the assembly of π-conjugated oligopeptides

We began by studying the effects of kinetics on the structural, electronic, and mechanical properties of assembled synthetic oligopeptides (**Li et al., *ACS Appl. Mater. Interfaces*, 2017a**). In particular, we aimed to systematically study the equilibrium self-assembly of synthetic oligopeptides with π-conjugated cores to understand the role of the kinetics on the process of acid-triggered assembly. In brief, protonation of individual peptides containing aspartic acid residues was found to trigger the assembly of these materials into 1-D fibers, with macromolecular assemblies stabilized by beta-sheet formation and π-stacking in the aromatic cores. However, the mechanism for the assembly process and the role of kinetics in determining assembled supramolecular structures is generally unknown.

We hypothesized that the rate of amino acid protonation relative to the rate of peptide diffusion is a key factor in determining the emergent structural properties of assembled materials. To control the kinetics of the self-assembly process, we developed an approach using organic liquids as isolation layers for mediating proton transport (**Figure 1**). In this process, the diffusion rate of acidic vapor into peptide monomer solutions can be tuned by varying the thickness (and identity) of the organic layer. In this way, we observed that the pH of the peptide monomer solution decreases at controllable (and generally much slower) rates compared to bulk solution addition of H^+. Notably, any organic liquid that is immiscible with water (and less dense than water) can be utilized as organic isolation layer. In general, we found that higher density organic liquids result in slower diffusion rates of acid vapor through the organic layer, though trace solubility of acid likely plays a role as well. As a proof-of-principle demonstration of this approach, we studied the self-assembly of a synthetic oligopeptide with a quaterthiophene core flanked by symmetric amino acid sequences with four residues (HO-Asp-Phe-Ala-Gly-quaterthiophene-Gly-Ala-Phe-Asp-OH, abbreviated as DFAG-4T). Interestingly, SEM images of self-assembled DFAG-4T fiber networks show that the morphology of the final assembled structure is influenced by the kinetics of self-assembly process (**Figures 1b-c**). In particular, slower rates of self-assembly (tuned by the organic layer) generally yield more highly ordered supramolecular structures with composed of pristine anisotropic fibers (**Figure 1c**) compared to faster rates of assembly with no control (**Figure 1b**).

As part of this effort, we developed a full analytical reaction-diffusion model to quantitatively describe the triggered assembly process. Our model provided invaluable insight into the mechanism of oligopeptide assembly, in particular whether assembly occurred in a reaction-dominated or diffusion-dominated regime (**Figure 2**). These regimes can be described by a dimensionless group called the Damkohler number *Da*, which gives the relative rates of reaction to diffusion. In the reaction-dominated regime, acid will accumulate at the organic/aqueous interface, thereby resulting in local and rapid peptide assembly near an assembly front. Consequently, the assembly front will propagate from the outside to the inside of the droplet, yielding ring-like pattern during the self-assembly process (shown experimentally in **Figure 2a**

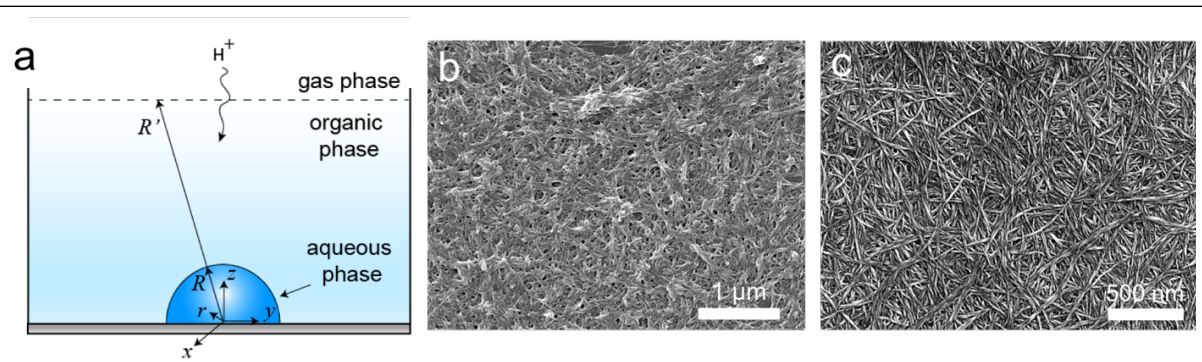

Figure 1: Non-equilibrium self-assembly of π-conjugated synthetic peptides. In a series of experiments, we tuned the assembly kinetics of π-conjugated oligopeptides to occur under reaction-dominated or diffusion-dominated conditions. (a) Schematic illustration of the experimental setup using an organic isolation layer for acid vapor diffusion. (b) and (c) Scanning electron microscopy (SEM) images of self-assembled DFAG-4T fibers without and with organic layer isolation, respectively.

with corresponding analytical results in **Figure 2c**). On the contrary, in the diffusion-dominated regime, the pH of the aqueous solution will decrease in a homogeneous fashion, thereby leading to spatially homogeneous self-assembly (shown experimentally in **Figure 2b** with corresponding analytical results in **Figure 2d**). In brief, results from the analytical model agree well with experimental results on peptide assembly, and this approach can be used for designing and engineering non-equilibrium assembly protocols for supramolecular assemblies. Finally, we applied the organic isolation layer method to study the assembly of several different materials, including the assembly of synthetic peptides containing non-sequence-defined amino acids (random primary sequence of amino acids comprised of leucine/glutamate repeats) linked to perylene diimide (PDI) cores. Interestingly, we found that PDI peptides with random sequences only yield 'bulb-like' assembled structures regardless of the rate of assembly, with no 1-D fibers. These results show that the chemical structure of peptide plays a crucial role in the final assembled morphology, regardless of kinetics. For these reasons, we moved on to studying the role of the underlying chemical structure (core and flanking amino acid sequence) in determining the structural properties of assembled materials.

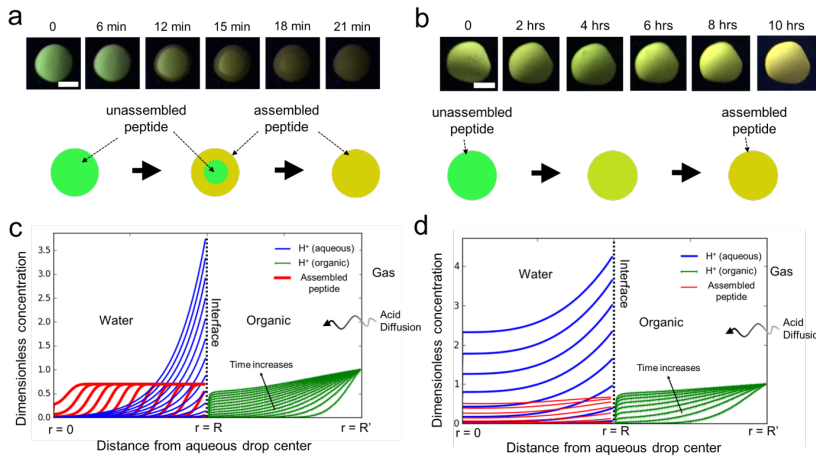

Figure 2: Reaction-controlled and diffusion-controlled assembly of π-conjugated oligopeptides using experiments and analytical modeling. (a) Optical micrographs of an aqueous DFAG-4T droplet undergoing assembly using toluene as the organic isolation layer. Under these conditions, reaction is rapid and an assembly front is observed, as shown in the schematic. (b) Optical micrographs of an aqueous DFAG-4T droplet undergoing assembly using silicone oil as the organic isolation layer. Under these conditions, the assembly reaction is substantially slowed and no assembly front is observed, thereby yielding spatially homogeneous assembly as shown in the schematic. (c) Results from the coupled reaction-diffusion analytical model for reaction-dominated assembly (Damkohler number Da = 1000). (d) Results from the reaction-diffusion model for diffusion-dominated assembly (Da = 0.1).

Thrust 2: Role of chemistry on the structural and optical properties of assembled materials

We next conducted a series of experiments to understand the role of the chemical identity of both the π-conjugated cores and flanking peptide sequences on the structural and optical properties of assembled materials. **Table 1** shows a summary of the sequence-defined materials studied in this funded project. From a broad view, the ultimate goal is to use directed assembly methods to tune the emergent properties of these materials. To this end, we also aimed to understand the role of chemistry on the overall assembly process.

Role of size of π-conjugated cores on assembly. We are investigating the role of the size of the functional cores on the assembled structures using synthetic peptides with systematically increasing numbers of thiophene units in the core (n=3,4,5,6). For these molecules, the core length was varied while keeping the same flanking peptide sequence (DADDG-3T, DADDG-4T, DADDG-

Chemical structure	Code
HO-DADDG-terthiophene-GDDAD-OH	DADDG-3T
HO-DADDG-quaterthiophene-GDDAD-OH	DADDG-4T
HO-DADDG-pentthiophene-GDDAD-OH	DADDG-5T
HO-DADDG-sexithiophene-GDDAD-OH	DADDG-6T
HO-DFAG-quaterthiophene-GAFD-OH	DFAG-4T
HO-DFAG-oligo(p-phenylenevinylene)-GAFD-OH	DFAG-OPV3
HO-DFAG-perylene diimide-GAFD-OH	DFAG-PDI

Table 1. Sequence-defined peptides used for probing the role of chemistry on the structural properties of assembled materials.

5T and DADDG-6T, chemical structures shown in **Figure 3a**, materials obtained from JD Tovar, Hopkins). Interestingly, we observed distinct assembled structures and fluorescence emission spectra for the four different peptides with variable length oligothiophene cores (**Figure 3b-e**). For DADDG-3T monomers, we observed clear 1-D fiber-like assembled structures with a bathochromic-shifted fluorescence emission (**Figure 3b**), which likely arises due to π-π stacking of the 3T cores. In contrast, both DADDG-5T and DADDG-6T (**Figures 3d and 3e**) show isotropic assembled structures upon assembly, albeit with a hypsochromic-shifted fluorescence emission, which is suggestive of internally self-twisted thiophene cores within the assembled structures. Moreover, the self-assembled structure of DADDG-4T showed the coexistence of both isotropic bulk-like structures and fiber structures, with the fluorescence emission spectrum showing both a hypsochromic-shifted and a bathochromic-shifted peak. The behavior of the DADDG-4T materials appears intermediate in response compared to the 3T and 5T / 6T materials. This work is currently being prepared for publication (**Jira et al., in preparation, 2018**).

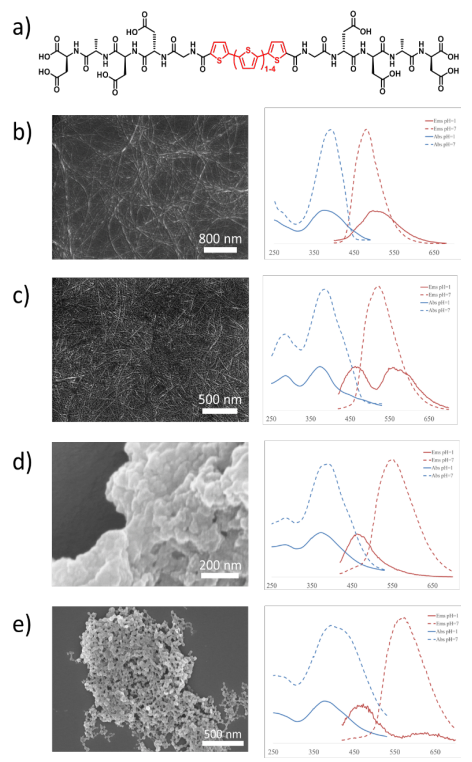

Figure 3. Probing the impact of pi-conjugated core chemistry on the structure of assembled materials. a) Chemical structure of DADDG-3T, 4T, 5T and 6T (*n*=1,2,3,4). b)-e) SEM images of self-assembled structures (left) and absorption (blue) and quenched fluorescenve emission spectra (red) before (pH =7, dashed) and after assembly (pH =1, solid) of b) DADDG-3T, c) DADDG-4T, d) DADDG-5T and e) DADDG-6T.

Role of chemical identity of pi-conjugated cores on assembly. We further studied the influence of the chemical identity of the cores on the self-assembly process. It is thought that aromatic cores assemble due to favorable π-π stacking interactions, mediated by H-bonding in the flanking sequences. We aimed to probe this general hypothesis by specially designing synthetic peptides with *different* aromatic cores (OPV3, 4T, and PDI) while maintaining the *same* flanking peptide residues. Following assembly, we performed a series of experiments to study the structural properties of these materials. Interestingly, our results show that different levels of protonation are required to trigger the assembly of oligopeptides with different cores (with same amino acid sequences) (**Figure 4**). These results are suggestive of an energy barrier (or higher repulsion force) between the cores during the self-assembly process, such that the protonation of peptide residues helps to overcome this barrier under acidic conditions. Fluorescence emission spectra of peptide solutions under different pH values (**Figure 4**) shows that the critical pH value for self-assembly of DFAG-4T, DFAG-OPV3, and DFAG-PDI was pH=5, 3.5, and 3, respectively, indicating that benzene rings may exhibit a higher energy barrier than thiophene. Moreover, higher levels of aromatic rings result in an increased energy barrier for self-assembly. Further scrutiny of the fluorescence emission spectrum of DFAG-PDI shows that the peptide assembled first (at pH around 4) with the decrease of the pH of the solution, thereby resulting in the quenching of fluorescence emission. However, the fluorescence emission peak shows a bathochromic shift for pH < 3, suggesting that π-stacking of the PDI cores required protonation of peptides.

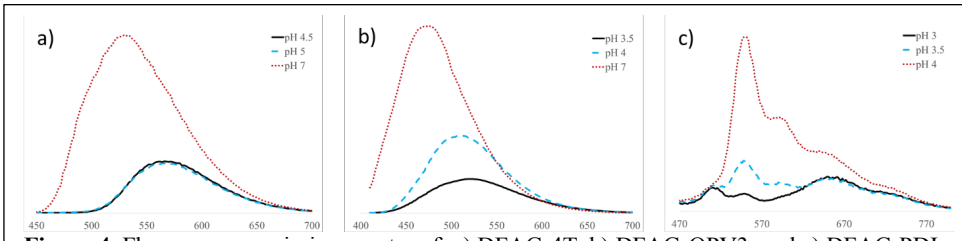

Figure 4. Fluorescence emission spectra of: a) DFAG-4T, b) DFAG-OPV3, and c) DFAG-PDI as a function of solution pH. Intensity as a function of emission wavelength (nm).

Thrust 3: *In situ* monitoring of the assembly process & sol-gel transition of π-conjugated oligopeptides

In Thrust 1, we found that the kinetics of self-assembly affects the emergent properties of π-conjugated oligopeptides, but the molecular mechanisms underlying assembly are not yet fully understood. Therefore, we investigated the assembly process using *in situ* methods to probe the sol-gel transition of π-conjugated oligopeptides using a combination of structural and optical tools based on multiple particle tracking microrheology (PTM), confocal fluorescence microscopy, circular dichroism (CD), and cryo-electron microscopy (**Zhou et al., *ACS Cent. Sci.*, 2017**). Our results show that π-conjugated oligopeptides assemble into fiber-like structures upon increasing oligopeptide concentration under aqueous, pH-neutral conditions, even in the absence of electrostatic screening of charged amino acid residues. Microrheology and optical spectroscopy reveal a critical fiber formation concentration (c_{fiber} = 0.1 mg/mL) and a critical gel concentration (c_{gel} = 1 mg/mL) for quaterthiophene peptides (DFAG-4T), as well as a critical diffusive exponent $\alpha_{crit} = 0.78 \pm 0.04$ for the onset of gelation. Based on the mean-squared displacements (MSDs) of probe particles in DFAG-4T solutions, we found that embedded probe particles exhibited Fickian diffusion with a diffusive exponent α = 1, characteristic of a simple Newtonian liquid at low peptide concentrations (0.025 mg/mL to 0.1 mg/mL), suggesting isolated peptides or small aggregates are suspended in an aqueous solvent at fairly low concentrations (**Figure 5a**). As the peptide concentration increases above 0.1 mg/mL, α begins to deviate from a value of unity, such that sub-diffusive behavior is observed to occur for peptide concentrations above 0.1 mg/mL, indicating oligopeptides begin to assemble into fibers. The diffusive exponent α for DFAG-4T drops dramatically when peptide concentration exceeds 1 mg/mL, which is suggestive of the onset of gelation. In order to probe the sol-gel transition, we performed a time-cure superposition (TCS) analysis to determine the critical exponent α_{crit} for DFAG-4T. As shown in **Figure 5b**, the master curve converges with a terminal of logarithmic slope $\alpha_{crit} = 0.78 \pm 0.04$, which is defined as the critical exponent at the gel point. For diffusive exponents $\alpha > \alpha_{crit}$, π-conjugated oligopeptides are in a sol phase, wherein small fibers are suspended in a viscous solvent without forming a network. For diffusive exponents $\alpha < \alpha_{crit}$, peptides are in a gel phase, wherein self-assembled fiber structures form a percolated network spanning the entire system.

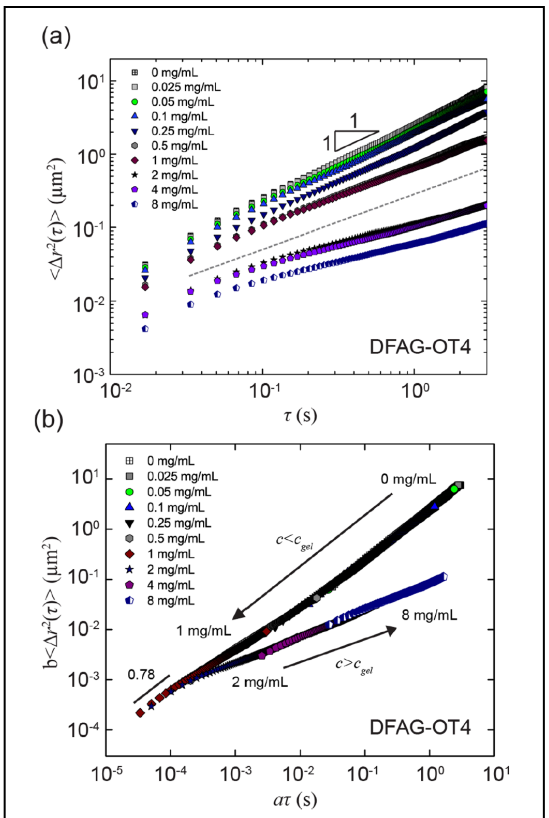

Figure 5. Microrheology of the sol–gel transition for DFAG-4T. (a) Ensemble-averaged MSDs $\langle \Delta r^2(\tau) \rangle$ versus lag time τ for probe particles in DFAG-4T solutions at different peptide concentrations. The dashed line shows the slope for the critical diffusive exponent α_{crit} = 0.78. (b) Time-cure superposition (TCS) of the MSD for DFAG-4T as a function of oligopeptide concentration. The master curve converges with a critical exponent $\alpha_{crit} = 0.78 \pm 0.04$ at the critical gel concentration c_{gel} = 1 mg/mL.

To further scrutinize the self-assembly behavior of π-conjugated oligopeptides, we studied the concentration-dependent assembly of DFAG-4T at neutral pH by combining PTM, confocal fluorescence microscopy, CD, and electron microscopy (**Figure 6**). For peptide concentrations $c > c_{gel}$, the diffusive exponent $\alpha \approx 0.5$, which suggests that the assembled DFAG-4T material is comprised of a percolated gel network. In addition, we probed the fluorescence emission spectra to track the progression of π–π stacking interactions in the π-conjugated cores at different stages of assembly. Interestingly, the peak fluorescence emission wavelength exhibits a bathochromic shift upon increasing peptide concentration (**Figure 6a**). The

red-shifted fluorescence emission is also evident in confocal fluorescence microscopy images of aqueous droplets of DFAG-4T, especially at the edge of the droplets (**Figure 6c**). The red shift in fluorescence emission wavelength suggests a face-to-face molecular ordering of OT4 cores that can be associated with classic H-aggregation. For $c > c_{gel}$, the fluorescence emission wavelength red-shifts more than 60 nm. To further probe the molecular-scale ordering of DFAG-4T during assembly, we performed CD measurements of DFAG-4T as a function of increasing peptide concentration at neutral pH (**Figure 6b**). For peptide concentrations $c > c_{fiber}$, CD absorption spectra show a broad minimum that shifts toward 218 nm, which is characteristic of β-sheet formation. Notably, CD data show that peptide subunits self-assemble toward a β-sheet-rich structure for peptide concentrations $c_{fiber} < c < c_{gel}$, which occurs before the onset of the sol-gel transition at c_{gel}. Therefore, CD spectra confirm that oligopeptide interactions gradually give rise to hydrogen-bonded structures upon increasing peptide concentration, likely due to interactions between adjacent peptide flanking sequences, which occurs before the onset of gelation. Finally, we performed cryo-electron microscopy on the assembled DFAG-4T materials. Scanning electron microscopy (SEM) images obtained from freeze-dried DFAG-4T solutions (2 mg/mL) directly reveal the existence of interlaced 3D percolated networks with an average mesh size ≲1 μm (**Figure 6d**). Moreover, probe particle trajectories are well described by Gaussian statistics, which suggests that the materials remain homogeneous before and after the sol–gel transition. Taken together, the combined microrheology–spectroscopy approach is quite powerful in elucidating the structural and optical properties of π-conjugated oligopeptides, thereby illuminating the fundamental self-assembly mechanisms for synthetic π-conjugated oligopeptides in solution.

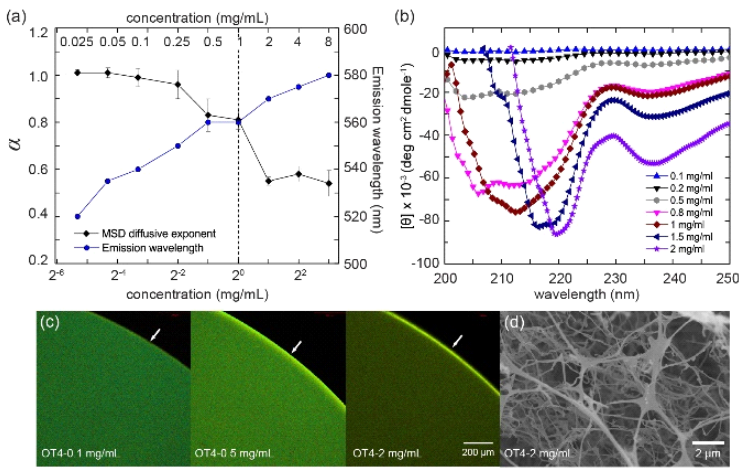

Figure 6. Assembly of DFAG-4T using a combination of microrheology, optical spectroscopy, and cryo-electron microscopy. (a) Diffusive exponent α from MSDs and peak fluorescence emission wavelength as functions of peptide concentration for DFAG-4T. Error bars for the diffusive exponent denote the standard deviation from multiple measurements. (b) CD spectra of DFAG-4T as a function of peptide concentration. (c) Confocal fluorescence microscopy images of DFAG-4T droplets at different peptide concentrations. Arrows indicate the edge of the droplet. (d) Cryo-SEM image of freeze-dried DFAG-4T solution at 2 mg/mL.

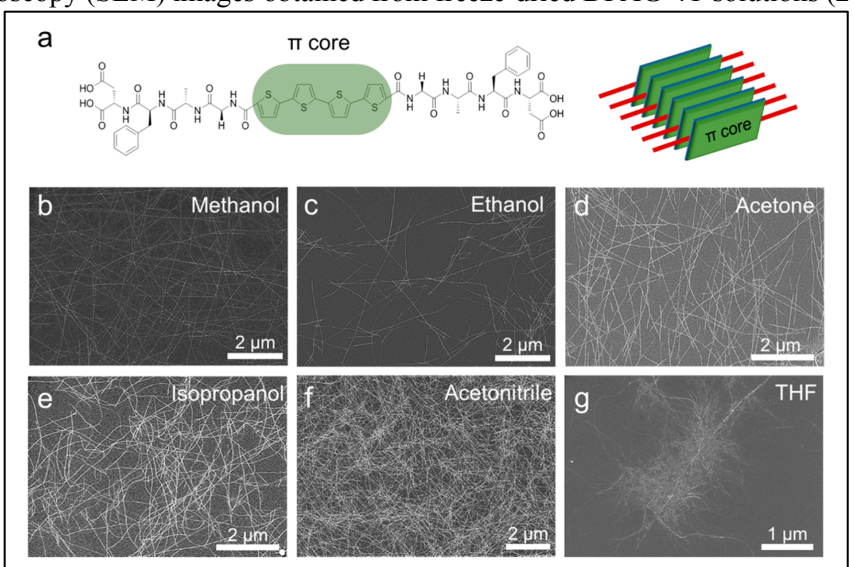

Figure 7. Evaporative self-assembly of π-conjugated oligopeptides. (a) Chemical structure of π-conjugated oligopeptide (DFAG-4T) and schematic illustration of 1-D self-assembly mediated by hydrogen bonding of peptide side chains and π–π stacking interactions within aromatic cores. (b–g) Scanning electron microscopy (SEM) images of self-assembled DFAG-4T fibers formed by rapid evaporative self-assembly using a variety of organic solvents.

Thrust 4: Colloidal templating method for macroscopic alignment and assembly of π-conjugated oligopeptides

As discussed in Thrust 3, we found that π-conjugated oligopeptides self-assemble into 1-D supramolecular fiber networks upon increasing the concentration of oligopeptide in aqueous solution – even at neutral pH. Capitalizing on this observation, we next demonstrated that solvent evaporation can provide an alternative pathway to trigger self-assembly. In particular, we developed a facile strategy to assemble and align supramolecular fibers over millimeter-sized length scales by confining evaporative assembly of π-conjugated oligopeptides inside colloidal microchannels (published in **Li et al., *ACS Appl. Mater. Interfaces*, 2017b**).

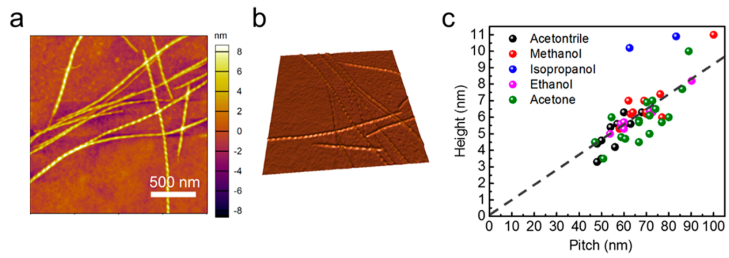

Figure 8. AFM imaging of 1-D assembled DFAG-4T fibers. (a) AFM images of assembled DFAG-4T fibers showing helical structures. (b) 2-D AFM height images of DFAG-4T fibers assembled using the evaporative assembly method on a solid surface using methanol as solvent (image size 2 × 2 μm). (c) Height and pitch relationship of helical DFAG-4T fibers using evaporative assembly in different organic solvents.

Evaporative assembly of π-conjugated oligopeptides: SEM and AFM. We found that common polar solvents such as methanol, ethanol, acetone, isopropanol, and acetonitrile yield discrete supramolecular fibers of DFAG-4T upon evaporation. Scanning electron microscopy (SEM) was used to characterize the structural properties of DFAG-4T fibers using the evaporative assembly method. SEM images of assembled DFAG-4T peptides show discrete fibers following evaporative assembly using methanol, ethanol, acetone, isopropanol, and acetonitrile (**Figures 7b-f**). In addition, two-photon confocal microscopy results showed that DFAG-4T fibers assembled using evaporative assembly exhibited similar π–π stacking interactions between quaterthiophene cores relative to acid-induced assembly. Notably, using THF as a solvent for evaporative assembly, a large amount of unassembled DFAG-4T peptide was observed in SEM (**Figure 7g**), confirmed by the fluorescence emission spectra with some local areas showing a fluorescence emission peak around a wavelength of 500 nm. We also found that the dipole moment of the polar solvent used for evaporative assembly likely plays a role in inducing oligopeptide self-assembly because the peptide residue interactions can be affected by solvent polarity.

We further studied the solvent effects on the conformation of assembled π-conjugated oligopeptides using atomic force microscopy (AFM) (**Figure 8**). Interestingly, these results show that DFAG-4T assembles into helical fibers by evaporative self-assembly, and the helical pitch of fibers is impacted by the selection of solvent for evaporative assembly. We found an approximately linear relationship between the pitch and height of assembled helical fibers, as shown in **Figure 8c**.

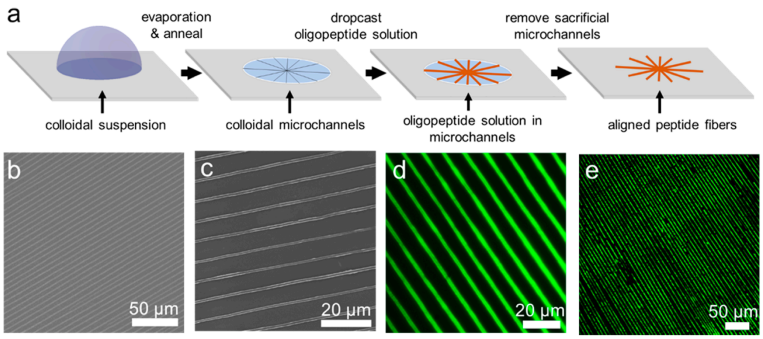

Figure 9. Assembly and alignment of π-conjugated oligopeptides using a colloidal microchannel templating method. (a) Schematic illustration of method to prepare colloidal microchannels, followed by evaporative assembly of oligopeptides and removal of sacrificial microchannels. (b) SEM image of highly ordered colloidal microchannels. (c) SEM image and (d,e) fluorescence emission images of aligned DFAG-4T fibers after removal of the sacrificial colloidal microchannel template.

Colloidal templating method for large-area assembly. We next demonstrated a facile strategy to assemble and align supramolecular

fibers over millimeter-sized length scales by confining evaporative assembly of π-conjugated oligopeptides inside colloidal microchannels. In these experiments, evaporative assembly of DFAG-4T was performed on solid substrates containing highly ordered colloidal microchannels as templates for peptide assembly (**Figure 9a**). Colloidal microchannels are created by simply drying a colloidal on a silicon wafer at 55 °C, which results in the generation of a colloidal film over large areas containing ordered microchannels due to capillary stress gradients (**Figure 9b**). After thermal annealing and preparation of colloidal microchannels, a solution of DFAG-4T peptide flowed through the channels via capillary forces and self-assembly of DFAG-4T peptide was confined within the channels. The sacrificial microchannel film was removed using a selective organic solvent (toluene) that preferentially dissolves polystyrene but is immiscible with DFAG-4T. Following removal of the sacrificial microchannels, a large array of DFAG-4T fibers with long-range ordering was obtained (**Figure 9c**). Two-photon fluorescence microscopy was used to characterize DFAG-4T fibers assembled using the microchannel templating method (**Figure 9d,e**), which revealed high degrees of alignment over relatively large areas. Moreover, we used two scanning probe spectral imaging techniques, AFM–IR imaging and photoinduced force microscopy (PiFM) to characterize the chemical and structural properties of DFAG-4T fibers. AFM–IR measurements on individual DFAG-4T deposited structures show a strong IR absorption at wavelength of 1650 cm^{-1}(**Figure 10a,b**), which can be attributed to the amide I absorption band in beta-sheet rich structures of assembled DFAG-4T fibers. PiFM results showed clear enhanced polarization at the assembled structure edges.

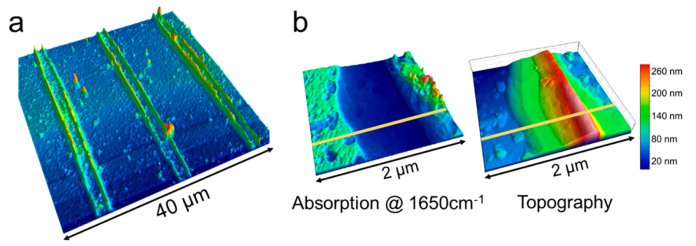

Figure 10. Nanoscale infrared spectroscopy-atomic force microscopy imaging of assembled fibers. (a) AFM–IR spectroscopy showing absorption at 1650 cm^{-1}. (b) AFM–IR absorption at 1650 cm^{-1} and AFM height profiles of the yellow line in (a). (c) Current–voltage (I–V) measurements of DFAG-4T using interdigitated array (IDA) electrodes. The bias was ramped from −10 to 10 V over multiple iterations (I1–I5) before and after applying 100 V (I6–I7). After application of high voltage, the I–V curves show a dramatic change, suggesting structural rearrangements under high bias.

Charge transport properties of assembled fibers. The charge transport properties of assembled DFAG-4T were further characterized using interdigitated electrodes. We deposited DFAG-4T fibers onto interdigitated array (IDA) electrodes with 2 µm channel length using evaporative assembly in methanol. Following fiber deposition, we measured the current–voltage (I-V) response in a two-point-probe geometry (**Figure 11a**). Nonlinear I-V curves were obtained by sweeping the applied bias from −10 to 10 V. The overall structures of these I–V curves are reminiscent of semiconductor junctions, which can be rationalized by considering the Schottky barriers. Moreover, a hysteresis loop in I-V curves was observed in these measurements, though this could arise due to several effects such as interfacial charge traps. Notably, the conductivity of DFAG-4T fibers was observed to be stable across multiple voltage sweep trials, such that the conductivity of DFAG-4T fibers remained unchanged during multiple cycles of applied bias between −10 to 10 V. However, when the applied voltage was increased above 40 V, repeated I-V measurements resulted in a continuous decrease in conductivity. These results indicate that self-

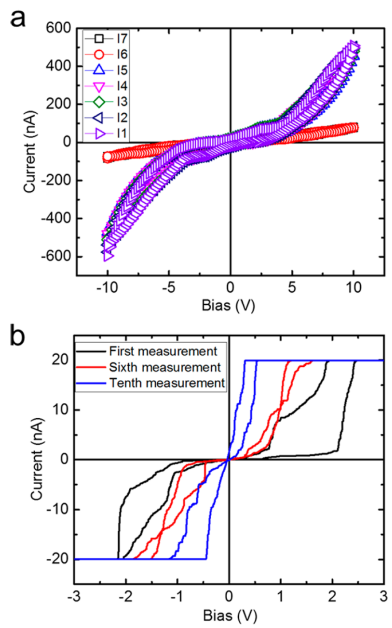

Figure 11. Electronic properties of assembled fibers. (a) Current–voltage (I–V) measurements of DFAG-4T using interdigitated array (IDA) electrodes. The bias was ramped from −10 to 10 V over multiple iterations (I1–I5) before and after applying 100 V (I6–I7). After application of high voltage, the I–V curves show a dramatic change, suggesting structural rearrangements under high bias.

assembled DFAG-4T fibers are not stable under high applied bias, which may be attributed to joule heating that could jeopardize the self-assembled oligopeptide fibers. After scanning the I-V curve across a high voltage range (100 V), the conductivity of DFAG-4T fibers reduced and could not be recovered under repeated measurements of sweeping the bias between −10 and 10 V (**Figure 11b**).

Summary

In summary, the funded DOE BES project has resulted in major strides in our understanding of the assembly mechanisms and structural and electronic properties of bio-hybrid materials, with a particular focus on π-conjugated oligopeptides. We developed and applied a wide range of methods including new cutting-edge experimental characterization tools (photo-induced force microscopy or PiFM, nano-IR, AFM-IR), *in situ* microrheological and combined spectroscopic analysis, theoretical modeling, new routes for solution processing (colloidal templating), and device design and optimization for mesoscale materials synthesis. From a broad perspective, achieving precise control of supramolecular assembly of bio-hybrid molecules holds to the potential to impact new advanced in many disciplines including chemistry, physics, and materials science. Taken together, our work has laid the basic scientific foundations for developing more complex assembled materials based on hybrid peptide/synthetic polymer conjugates with desired control over the structure and electronic properties of these materials.